depending on the Reynolds number, while the corresponding differences are 13–19% for the fixed pressure drop condition. The weak dependence of the results on S_L/D_f suggests that they can be regarded as universal (i.e. independent of S_L/D_f) in the investigated range.

The near coincidence of the Q_I/Q_S values for the $T_x = T_\infty$ and $T_x = T_{mix}$ models appears to lend credence to the superior performance of the in-line array. However, it can be argued that both models are unfair to the staggered array. To neutralize this concern, Q_I corresponding to the $T_x = T_{mix}$ model will be compared to Q_S for the $T_x = T_\infty$ model, thereby penalizing the in-line array since $(\overline{T_b - T_{mix}})$ is smaller than $(\overline{T_b - T_\infty})$. The ratio $Q_I(T_{mix})/Q_S(T_\infty)$ is plotted in Fig. 4. Although the Q ratios in Fig. 4 are closer to unity than those of Fig. 3, Q_I continues to exceed Q_S. Thus, for the investigated cases, it appears advantageous to use in-line deployment in preference to staggered deployment.

REFERENCE

1. E. M. Sparrow and F. Samie, Heat transfer and pressure drop results for one- and two-row arrays of finned tubes, *Int. J. Heat Mass Transfer* **28**, 2247–2259 (1985).

Int. J. Heat Mass Transfer. Vol. 28, No. 12, pp. 2382–2385, 1985
Printed in Great Britain

0017-9310/85 $3.00 + 0.00

Countercurrent flow limits for steam and cold water through a horizontal perforated plate with vertical jet injection*

I. DILBER and S. G. BANKOFF†
Chemical Engineering Department and Mechanical and Nuclear Engineering Department, Northwestern University, Evanston, IL 60201, U.S.A.

(*Received* 15 *August* 1984 *and in final form* 28 *May* 1985)

INTRODUCTION

IN A POSTULATED loss-of-coolant accident in a light-water nuclear reactor, emergency core cooling system water may be injected into the upper plenum above the upper tie plate. However, penetration of this water downwards into the core can occur only when the steam rising from the overheated core drops below a critical flooding velocity. This flooding phenomenon has been studied in various geometries [1, 2]. Bankoff *et al.* [3] determined the points of zero and complete water delivery for steam–water and air–water countercurrent flow through horizontal perforated plates, using a horizontal spray for the injected water. The present study is an extension of this work, in which a vertically downwards water jet at various elevations above the plate is employed. Significantly increased penetration capabilities are found, pointing towards the possibility of improved core cooling and lower peak clad temperatures.

EQUIPMENT AND PROCEDURE

The equipment, shown in Fig. 1, is essentially the same as in the previous experiments [3], except that here water is injected vertically downwards through a copper tube (I.D. 11.1 mm). The perforated plate contains 15 10.5-mm holes, giving a porosity of 0.423. The pool overflow is located 267 mm above the test plate. The water that penetrates through the plate is drained through the bottom outlet. The steam is injected downwards at a 45° angle to minimize entrance effects, and can flow out either with the water overflow or the steam outlet at the top of the channel.

Four heights of water injection above the test plate were employed: 356, 203, 51 and 0 mm. The water jet was directed towards the hole shown as shaded in the figure, except for the 0-mm case, when the tube was attached to the center hole. The water temperature varied between 0 and 12°C, and the mass flow rate from 0.023 to 0.491 kg s^{-1}. The steam was saturated, with a mass flow rate between 0.0074 and 0.0312 kg s^{-1}.

The zero-delivery point for a given inlet water flow rate is here defined as the point where downward liquid delivery just begins. It was determined visually by gradually increasing the steam flow rate until no delivery is observed through the plate. For the two lowest water injection heights, the water jet penetrated through the perforated plate before being turned around. In this case, zero-delivery corresponds to a negligible rate of change in the level of water accumulated at the bottom of the channel. The total-delivery point, on the other hand, is defined as the point where the steam flow rate just fails to maintain the water pool above the plate, so that a sudden collapse of the pool is observed.

DATA CORRELATION

For the correlation of countercurrent gas–liquid vertical flow, the Wallis [4] or Kutateladze [5] models have been employed. An interpolative scaling between these two has been given by Bankoff *et al.* [3] in the form:

$$H_g^{*1/2}/C + H_f^{*1/2}/C = 1. \quad (1)$$

The dimensionless flow rates are defined by:

$$H_i^* = [\rho_i/gw(\rho_f - \rho_g)]^{1/2} j_i; \quad i = \text{f or g}, \quad (2)$$

where j_i is the volumetric flux of the ith phase, and w is a length scale given by:

$$w = D_h^{(1-\alpha)}[\sigma/g(\rho_f - \rho_g)]^{\alpha/2}. \quad (3)$$

Geometrical effects are taken into account by choosing α to be of the form:

$$\alpha = \tanh(2\pi D_h R/t_p), \quad (4)$$

where D_h is the hole diameter, R is the porosity of the plate and t_p is the plate thickness. Following the correlation obtained by

* This work was supported by a contract with the U.S. Nuclear Regulatory Commission.
† To whom communications should be addressed.

NOMENCLATURE

C	empirical constant
C_p	specific heat
D_h	hole diameter
f	condensation efficiency
g	gravitational constant
H	dimensionless flow rate
h	enthalpy
h_{fg}	saturation enthalpy
$\dot{h}$	enthalpy rate
h_{in}	water injection height
I	parameter defined in equation (10)
j	volumetric flux
R	porosity
t_p	plate thickness
T	temperature
W	mass flow rate
w	length scale defined in equation (3).

Greek symbols

α	parameter defined in equation (4)
ρ	density
σ	surface tension.

Subscripts

d	delivery
e	effective,
f	liquid phase
fg	phase change
g	vapor phase
h	hole
i	evaluation at intersection point in equation (9)
in	inlet
sat	saturation condition.

Sun and Fernandez [6], for this geometry the value of the constant C in equation (1) is found to be 1.927.

Equation (1) was further modified [3] for steam–water flows to account for the condensation effects:

$$H_{g,e}^{*1/2}/C + H_{f,d}^{*1/2}/C = 1, \quad (5)$$

where the effective steam flow parameter is defined by:

$$H_{g,e}^{*} = H_{g}^{*} - f(\rho_f/\rho_g)^{1/2}(T_{sat} - T_f)C_p H_{f,in}^{*}/h_{fg}. \quad (6)$$

Here, $H_{f,in}^{*}$ and $H_{f,d}^{*}$ are the dimensionless water flow rates corresponding to inlet and downwards delivery through the plate; H_g^{*} is again the dimensionless inlet stream flow rate; h_{fg} is the saturation enthalpy of steam; f is a condensation efficiency, obtained from the slope of a plot (see Fig. 2) of the steam enthalpy rate, $\dot{h}_g$, vs the water enthalpy rate, $\dot{h}_f$, defined as:

$$\dot{h}_g = W_g h_g; \quad \dot{h}_f = W_f C_p (T_{sat} - T_f). \quad (7)$$

Here, W_g and W_f are the mass flow rates for steam and water, respectively. At the zero-delivery point equation (5) becomes:

$$H_{g,e}^{*1/2}/C = 1. \quad (8)$$

Equation (8) is good only for the cases where the data can be approximated by a single straight line with slope f, such as the high injection-height data. To correlate low injection-height data, where turn-around below the plate was observed, two straight lines, with slopes f_1 and f_2, were employed. For these cases the dimensionless effective steam flow rate parameter was redefined as:

$$H_{g,e}^{*} = H_{g}^{*} - f_1[IH_{f,in}^{*}]_i - f_2 I[H_{f,in}^{*} - (H_{f,in}^{*})_i], \quad (9)$$

where the subscript i indicates evaluation at the intersection point of the two lines, and I is given by:

$$I = [C_p(T_{sat} - T_f)/h_{fg}](\rho_f/\rho_g)^{1/2}. \quad (10)$$

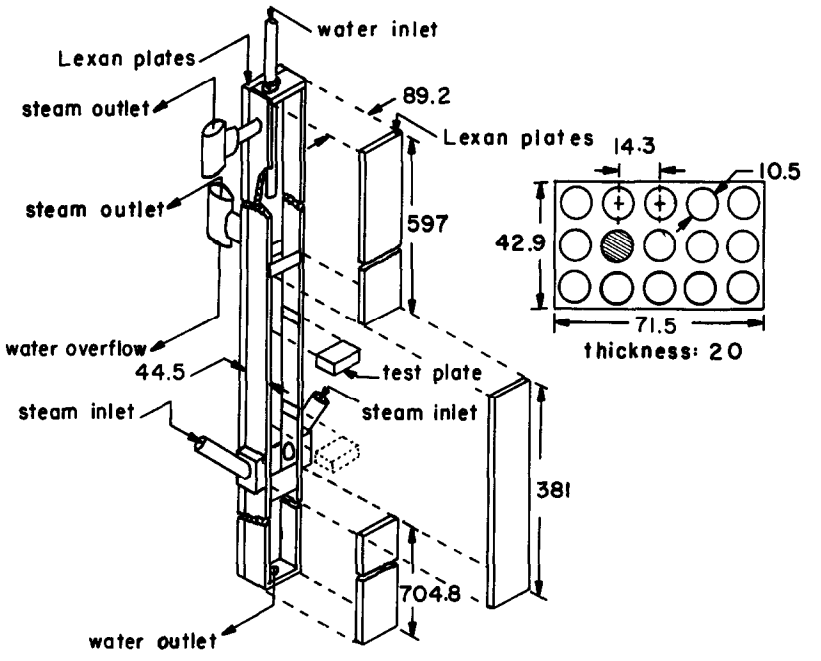

FIG. 1. The test channel and the perforated plate (dimensions in mm).

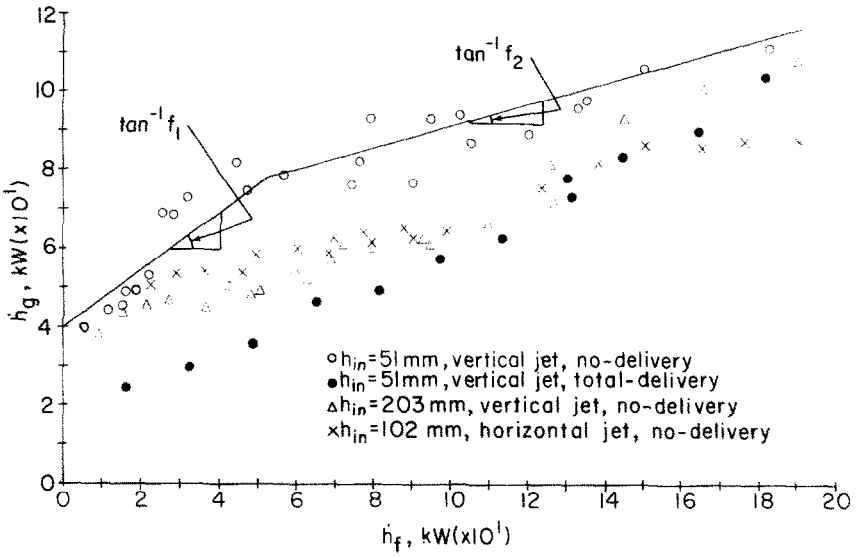

FIG. 2. Typical enthalpy rate data for vertical jet compared to similar horizontal spray data.

The point of intersection is empirically determined by fitting two straight lines to the data. Equations (6) and (9) are used to correlate data points up to and beyond the intersection. The second term in equation (9) represents the condensation up to the intersection point, and the last term represents the condensation from that point to the point of interest.

RESULTS AND DISCUSSION

For all runs the water inlet temperature was between 0 and 12°C. We note that, the water inlet temperature and the inlet tube diameter being fixed, the water enthalpy rate may be considered to be proportional to the jet momentum. However, neither the peak stagnation pressure nor the jet half width could be measured at the plate in the present equipment.

Typical enthalpy rate plots are shown in Fig. 2 for total- and no-delivery points. The slopes of the curves correspond to the condensation efficiencies used in equation (6) for that particular set of data. In most cases, the data can be approximated by a straight line, except for the case of low water injection heights, 51 and 0 mm (not shown), where the data are approximated by two straight lines. Data for the two highest water inlet positions (356 and 203 mm) showed no significant difference; hence, only one set of data is presented. For these cases the inlet water momentum has no effect on penetration, as shown by data for both horizontal and vertical jets. However, with a 51-mm injection height a substantial increase in steam enthalpy rate is required for zero-delivery, since the water jet penetrating through the plate condenses steam in the lower plenum in the process of being turned around. Furthermore, the presence of cold water near the plate results in sudden collapse of steam bubbles in or near the holes, causing downwards penetration of water. A similar behavior was observed at high water enthalpy rates, where the complete

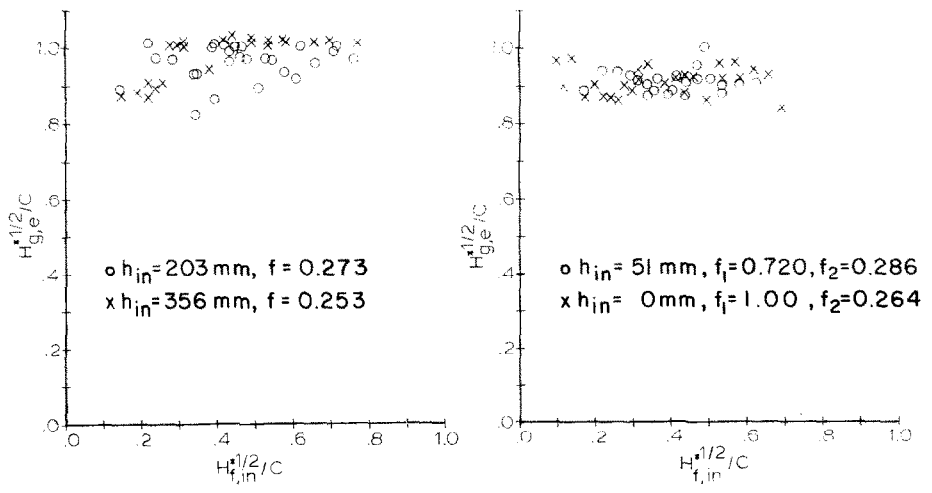

FIG. 3. Dimensionless steam flow rate for no-delivery point.

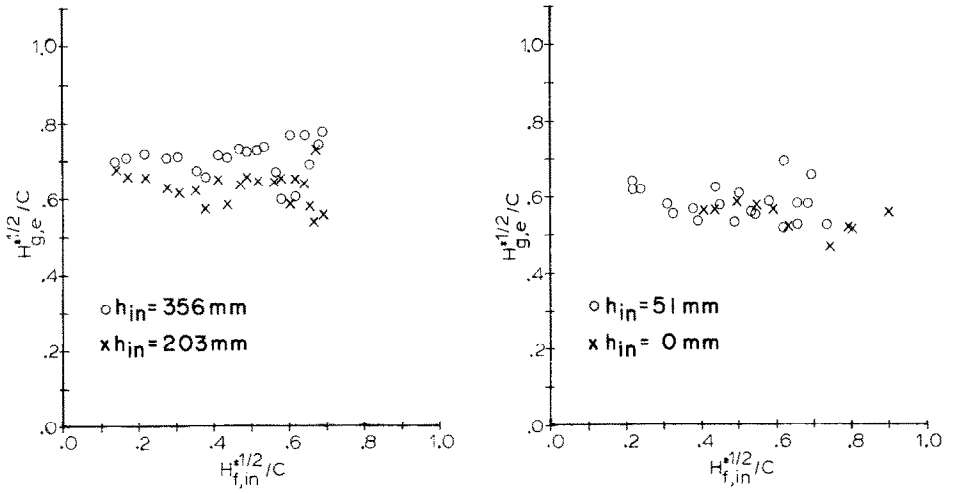

FIG. 4. Dimensionless steam flow rate for total-delivery point.

and zero penetration curves tended to intersect. Sudden collapses of the water pool were observed and the flow pattern switched back and forth between the two extremes. The data for 0 mm water injection [7] showed that even higher steam flow rates were required.

Equation (6) is used to correlate all the total delivery data and the no-delivery data for the two highest water inlet positions, 356 and 203 mm, and equation (9) is used for the no-delivery data of the two lowest water inlet positions, 51 and 0 mm. As shown in Fig. 3, the zero-penetration points are in good agreement with equation (8). Assuming that equation (6) is valid just before total dumping occurs, the complete-penetration data presented in Fig. 4 show a minimum value for the dimensionless steam flow rate parameter of about 0.6, which is independent of the value of the dimensionless water flow rate parameter.

It is therefore concluded that, for this particular rectangular geometry, intended to simulate the upper tie-plate of the German PKU reactor, vertical injection of cold water close to the tie-plate can be more efficient in cooling the reactor core, since delivery is observed for smaller water flow rates compared to horizontal spray experiments [3]. However, the importance of the condensation efficiency, f, for other geometries, as well as the effects of liquid subcooling, jet diameter and jet velocity at the plate, are subjects for further investigation.

REFERENCES

1. J. A. Block, P. H. Rothe, M. W. Fanning, C. J. Crowley and G. B. Wallis, Analysis of ECC delivery, CREARE TN-231 (March 1976).
2. T. Ueda and S. Suzuki, Behavior of liquid films and flooding in counter-current two phase flow. Part 2. Flow in annuli and rod bundles, *Int. J. Multiphase Flow* **4**, 157–170 (1978).
3. S. G. Bankoff, R. S. Tankin, M. C. Yuen and C. L. Hsieh, Countercurrent flow of air/water and steam/water through a horizontal perforated plate, *Int. J. Heat Mass Transfer* **24**, 1381–1395 (1981).
4. G. B. Wallis, *One Dimensional Two-phase Flow*. McGraw-Hill, New York (1969).
5. O. L. Pushkina and Y. L. Sorokin, Breakdown of liquid film motion in vertical tubes, *Heat Transfer—Sov. Res.* **1**, 56–64 (1969).
6. K. H. Sun, Flooding correlations for BWR bundle upper tie plates and bottom side-entry orifices, 2nd Multiphase Flow and Heat Transfer Symposium-Workshop, Miami Beach, Florida (1979).
7. I. Dilber, Counter-current steam/water flow above a perforated plate—vertical injection of water. M.S. thesis, Mechanical and Nuclear Engineering Department, Northwestern University, Evanston, Illinois (1981).

Int. J. Heat Mass Transfer. Vol. 28, No. 12, pp. 2385–2388, 1985
Printed in Great Britain

0017-9310/85 $3.00 + 0.00

Similarity between unsteady conduction and natural convection

M. G. DAVIES
Department of Building Engineering, The University, Liverpool L69 3BX, U.K.

(*Received* 20 *March* 1985 *and in final form* 26 *June* 1985)

1. INTRODUCTION

THE TRANSFER of heat by unsteady conduction through a solid—the wall of a room for example—and the process of natural convection that typically takes place between the air and the wall of a room, are physically speaking very dissimilar processes. Nevertheless, the analytical expressions for the heat flow at the surface due to the processes show some structural similarities as will be demonstrated below.

2. SINUSOIDALLY DRIVEN CONDUCTED HEAT FLOW

One-dimensional heat flow in a solid is subject to the equation

$$k\frac{\partial^2 T}{\partial x^2} = \rho c\frac{\partial T}{\partial t}. \quad (1)$$